miR-409-3p suppresses the proliferation, invasion and migration of tongue squamous cell carcinoma via targeting *RDX*

HUJIE CHEN and JING DAI

Department of Stomatology, Jingzhou Central Hospital, The Second Clinical Medical College,
Yangtze University, Jingzhou, Hubei 434000, P.R. China

Abstract. The aim of the present study is to investigate the role of microRNA (miRNA/miR)-409-3p in the proliferation, invasion and migration of tongue squamous cell carcinoma (TSCC) cells via targeting radixin (*RDX*) gene. The expression of miR-409-3p was detected by reverse transcription-quantitative polymerase chain reaction (RT-qPCR) in TSCC tissue and cell lines. The binding of miR-409-3p to *RDX* was investigated by performing a dual-luciferase reporter gene assay. Tca8113 cells were selected to transfect with miR-409-3p mimic/inhibitor, small interfering (si)-RDX, and miR-409-3p inhibitor + si-RDX, as well as negative control (NC) respectively. The proliferative, migratory and invasive abilities of transfected Tca8113 cells were investigated by cell-counting-kit-8, wound-healing and Transwell assays, respectively. Additionally, a tumor xenograft model was constructed to examine the effects of miR-409-3p on the tumor growth and lymphatic metastasis in nude mice. A significant downregulation was detected in miR-409-3p expression in TSCC tissues and cells (all P<0.05) compared with normal tongue mucosa tissues and cell line, which was associated with lymph node metastasis and tumor-node metastasis staging (both P<0.05). The results from the dual-luciferase reporter gene assay indicated that *RDX* is a potential target gene of miR-409-3p. Compared with the blank group, a marked reduction in RDX expression, cell proliferation, migration and invasion was detected in the miR-409-3p mimic group and si-RDX group (all P<0.05). Conversely, the reverse was observed in cells that were transfected with the miR-409-3p inhibitor. Furthermore, si-RDX is able to reverse the effect of miR-409-3p inhibitor on cell proliferation, invasion and migration (all P<0.05). The results form the tumor xenograft

model of nude mice verified that miR-409-3p mimic is able to inhibit the growth of Tca8113 tumor cells and lymph node metastasis in nude mice. miR-409-3p may delay the proliferation of TSCC cells by inhibiting of *RDX* so as to decrease its migratory and invasive abilities. Therefore, miR-409-3p may be a potential target for the clinical treatment of TSCC.

Introduction

As the most common malignancy of head and neck, oral squamous cell carcinoma (OSCC) ranks the top six of malignant tumors worldwide with unsatisfactory prognosis (1). Tongue squamous cell carcinoma (TSCC) is one of the leading subtypes of OSCC, which frequently results in the malfunction of mastication, speech and deglutition, with the characteristics of high degree of malignancy, high rate of tumor metastasis and high recurrence (2,3). Despite of surgery combined with chemoradiotherapy as the primary treatment for TSCC, postoperative recurrence and the rate of distant metastasis remain high and the total 5-year survival rate is only ~50~60%. This critically affects influencing the quality of life of patients (4-6). With the broad development of tumor marker and molecular targeted therapy (7), a more detailed understanding of the mechanisms contributing to the carcinogenesis of TSCC would be of value to improve the therapeutic effect of TSCC at the molecular level.

microRNA (miRNA/miR), a type of highly conserved non-coding small molecules, serves an important role in numerous biological activities by regulating the expression of the target mRNAs at the post-transcriptional level, giving rise to mRNA degradation or translational suppression (8-10). miRNA-409-3p, located on chromosome 14q32.31, has been demonstrated to regulate several cellular processes, including cell proliferation, apoptosis and metastasis (11). Notably, miR-409-3p was credited as a promising tumor suppressor to inhibit cell proliferation, invasion and migration by suppressing the target gene *c-Met* in lung adenocarcinoma (12) and bladder cancer (13). Similarly in gastric cancer, downregulation of miR-409-3p was apparent. The overexpression of miR-409-3p *in vitro* and *in vivo* may inhibit the target gene PHD finger protein 10 to restrict cell proliferation and accelerate apoptosis (14). However, Josson *et al* (15) identified elevated miR-409-3p/-5p levels in prostate cancer, thereby indicating that it may facilitate tumorigenesis,

Correspondence to: Mrs. Hujie Chen, Department of Stomatology, Jingzhou Central Hospital, The Second Clinical Medical College, Yangtze University, 1 Renmin Road, Jingzhou, Hubei 434000, P.R. China
E-mail: chen_chhj@163.com

epithelial-to-mesenchymal transition, as well as bone metastasis of prostate cancer. This suggests that miR-409-3p may serve important functions in different tumor progression, including TSCC.

Radixin (RDX) is a tumor-associated factor that belongs to the ezrin-radixin-moesin (ERM) family (16), which is involved in the regulation of diverse cellular functions, including cell morphogenesis and polarization, as well as adhesion and migration (17,18). Previous studies reported a close association of *RDX* with invasion and migration of tumor cells. As reported by Tsai *et al* (19), miR-196a/-196b may enhance the invasion and migration of gastric cancer cells by inhibiting the mRNA and protein expression of RDX. Additionally, with the assistance of target gene prediction website, it was demonstrated that *RDX* may be a potential target gene of miR-409-3p, but little evidence is available regarding the association between miR-409-3p and *RDX* in TSCC (20). Therefore, the aim of the present study was to investigate the effects of miR-409-3p on *RDX* in the development of TSCC and potential underlying molecular mechanisms, thereby providing the potential strategy to improve the diagnosis, intervention and treatment of TSCC.

Materials and methods

Ethics statement. The present study conformed to the criteria issued by the Declaration of Helsinki (21). All patients were informed, agreed to the experiment and signed informed consent forms, and the present study was granted permission from the Clinical Ethics Committee of Jingzhou Central Hospital (Hubei, China). All animal procedures were performed according to the Guide for the Care and Use of Laboratory Animals published by the US National Institutes of Health (22).

Study objects. A total of 68 patients, (38 males and 30 females; mean age, 57.18±9.77 years) treated with surgery and diagnosed as primary TSCC at the Department of Oral and Maxillofacial Surgery at Jingzhou Central Hospital from December 2014 to December 2016, were collected as case group. Inclusion criteria were as follows; histological diagnosis of TSCC confirmed on hematoxylin and eosin-stained sections. Exclusion criteria were as follows; immunosuppressed patients, patients who had previously been diagnosed with cancer (of any type and location), or patients who had previously undergone radiation therapy. Among the 68 patients, 42 cases were poorly and moderately differentiated and 26 cases were well differentiated. Lymph node metastasis was absent in a total of 48 cases and present in 20 cases. Of these patients, 49 cases were aged ≥55 years, and 19 cases were aged <55 years. According to the tumor-node metastasis (TNM) staging of World Health Organization (23), 43 cases were in stage I-II and 25 cases were in stage III-IV. Based on tumor diameter, 44 cases were ≥2 cm and 24 cases were <2 cm.

Additionally, samples from an additional 25 cases were obtained from the Department of Oral and Maxillofacial Surgery, Jingzhou Central Hospital (Jingzhou, China) consisting of 13 males and 12 females (mean age, 56.45±8.69 years) taken from non-neoplastic surgery of the tongue and confirmed as normal tongue mucosa tissues by routine pathological examination were selected as the normal control group. There were no statistical differences in terms of gender and age between the two groups of patients (both P>0.05). All specimens were immediately stored in liquid nitrogen.

Selection of cells and culture. The human oral keratinocytes (HOK) and human TSCC cell lines, including Tca8113, SCC9, SCC25, and Ca127, were purchased from the Type Culture Collection of the Chinese Academy of Sciences. Dulbecco's modified Eagle medium (DMEM, Gibco; Thermo Fisher Scientific, Inc., Waltham, MA, USA) containing 10% fetal bovine serum (FBS) (Invitrogen; Thermo Fisher Scientific, Inc.) and 1% penicillin-streptomycin (Gibco; Thermo Fisher Scientific, Inc.) were used for culture with 5% CO_2 at 37°C under a humidified atmosphere. The culture medium was replaced every 2 days or following the thawing of cells. When the cells were at a confluence of ~80~90% cell passaging was carried out. The cells in logarithmic phase were seeded in 6-well plate at a density of 5×10^3.

Reverse transcription-quantitative polymerase chain reaction (RT-qPCR). Total RNA was extracted from tissues and cells using Trizol reagent (Invitrogen; Thermo Fisher Scientific, Inc.). The optical density (OD) of RNA at 260 and 280 nm was determined by ultraviolet spectrophotometer, and RNA concentration was calculated. The RNA samples were stored at -80°C. On the basis of gene sequences published in Genbank, primers (Table I) were designed using Primer software (version 5.0; Applied Biosystems; Thermo Fisher Scientific, Inc.) and synthesized by Shanghai Biological Engineering Co., Ltd. (Shanghai, China) Total RNA reverse transcription PCR was performed according to the manufacturer's protocol (Takara Biotechnology Ltd., Dalian, China). PCR conditions consisted of pre-denaturation at 95°C for 15 min and 40 cycles of denaturation at 94°C for 15 sec and annealing/extension at 60°C for 30 sec. U6 was used as the internal reference control for miR-409-3p, and β-actin was employed as the internal reference control for RDX, $2^{-\Delta\Delta Cq}$ (24) was used to calculate the relative expression of the target gene (25). Each experiment was repeated three times.

Dual-luciferase reporter gene assay. TargetScan (www.targetscan.org) was used to predict the binding site of miR-409-3p and *RDX* 3'untranslated region (UTR). Then, wild-type (WT) *RDX* 3'UTR plasmid (named as *RDX* 3'UTR-WT) and mutated (MUT) *RDX* 3'UTR (named as *RDX* 3'UTR-MUT) were constructed. The target sequences were as follows; WT-*RDX*, 3'UTR is 5'-UUAAGGGAGCUC UUCAACAUUA-3' and MUT *RDX,* 5'-UUAAGGGAG CUCUUGTCGGAAA-3'. For the transfection experiments, the following were transfected separately into the Tca8113 cells: miR-409-3p mimics + RDX-WT, miR-409-3p mimics + RDX-MUT, miR-409-3p NC + RDX-WT and miR-409-3p NC + RDX-MUT. Lipofectamine® 2000 (Invitrogen; Thermo Fisher Scientific, Inc.) was used for transfection. The luciferase activity was detected by dual-luciferase reporter gene assay kit (Promega Corporation, Madison, WI, USA) following the manufacturer's protocol. The results were expressed as relative luciferase activity (firefly luciferase/*Renilla* luciferase). Each experiment was repeated three times.

Table I. Primer sequences for reverse transcription-quantitative polymerase chain reaction.

Gene	Sequences (5'-3')
miR-409-3p	
Forward	GAATGTTGCTCGGTGA
Reverse	GTGCAGGGTCCGAGGT
U6	
Forward	GCGCGTCGTGAAGCGTTC
Reverse	GTGCAGGGTCCGAGGT
RDX	
Forward	GAATCAGGAGCAGCTAGCAGCAGAACTT
Reverse	TTGGTCTTTTCCAAGTCTTCCTGGGCTGCA
β-actin	
Forward	CAAACTGAAGCTCGCACTCTC
Reverse	GCTGCAGATTCTTGGGTTGTG

miR, miRNA; RDX, radixin.

Cell grouping and transfection. Tca8113 cells at the logarithmic phase were divided into six groups, including blank (without any transfection), negative control (NC; 5'-ACTACTGAGTGACAGTAGA-3') (transfected with NC sequence), miR-409-3p mimic (transfected with miR-409-3p mimic sequence), miR-409-3p inhibitor (transfected with miR-409-3p inhibitor sequence), small-interfering (si)-RDX group (transfected with si-RDX) and miR-409-3p inhibitor + si-RDX group (transfected with miR-409-3p inhibitor and si-RDX) groups. miR-409-3p mimic/inhibitor was purchased from Applied Biosystems (Thermo Fisher Scientific, Inc.), while si-RDX was obtained from Guangzhou RiboBio Co., Ltd (Guangzhou, China). Cell transfection in each group was performed using Lipofectamine® 2000 (Invitrogen; Thermo Fisher Scientific, Inc.). Each experiment was repeated three times.

Western blotting. Total protein was extracted from each group, and protein concentration was determined using bicinchoninic acid assay kit (Beyotime Institute of Biotechnology, Haimen, China). With the addition of loading buffer, the extracted protein was heated at 95°C for 10 min and 30 μg protein was loaded on 10% polyacrylamide gel. Following the transfer of the proteins to a polyvinylidene (PVDF) membrane, the PVDF membrane was blocked with 5% bovine serum albumin (Sigma-Aldrich; Merck KGaA, Darmstadt, Germany) for 1 h at room temperature, and then was incubated with primary antibody against RDX (1:500; cat. no. ab52495; Epitomics; Abcam, Cambridge, UK) and β-actin (1:1,000; cat. no. A1978; Sigma-Aldrich; Merck KGaA) at 4°C overnight. Subsequently, PVDF membrane was washed by Tris-buffered saline with Tween-20 three times at room temperature (5 min per wash), followed by 1-h incubation with the corresponding horseradish peroxidase (HRP)-conjugated secondary antibody (1:1,000; cat. no. ab131368; Epitomics; Abcam, Cambridge, UK) at room temperature. Following an additional washing step, PVDF membrane was developed using chemiluminescence reagent (GE Healthcare, Chicago, IL, USA) and analyzed by Bio-Rad Gel Doc EZ imager (Bio-Rad Laboratories, Inc., Hercules, CA, USA) with β-actin as an internal reference. Each band was analyzed using the Image Pro Plus 6.0 (Olympus, Tokyo, Japan). Each experiment was repeated three times.

CCK-8 assay. The cells at the logarithmic phase were collected from each group, made into cell suspension and added into a 96-well plate at 100 μl/well. Each group was provided with 3 parallel control wells. The cells were cultured at 37°C with 5% CO_2 for 24, 48 and 72 h respectively. An additional 1-h incubation in each well was performed with the addition of 10 μl Cell Counting Kit-8 (CCK-8) (Dojindo Molecular Technologies, Inc., Kumamoto, Japan). The microplate reader (Thermo Fisher Scientific, Inc.) was used to determine the OD at 450 nm. Every experiment was repeated three times using the mean OD value.

Scratch wound-healing assay. Tca8113 cells were seeded in a 6-well plate at a density of 5×10^4. After reaching from 70-80% confluence, a cell scraper (width, 2 mm) was used to the scratch cells. The cells were observed at 0 and 48 h and imaged using an IX71 inverted microscope (Olympus), and Image-Pro Plus 6.0 software was used to measure the distance between the scratches. The cell migration distance was calculated using the following equation: Cell migration distance (mm)=(scratch distance at 0 h)-(scratch distance at 48 h). Each experiment was repeated three times.

Transwell invasion assay. Matrigel basement membrane matrix (BD Biosciences, Franklin Lakes, NJ or San Jose, CA, USA) was thawed at 4°C. Briefly, 5×10^4 cells in serum-free media were placed into the upper chamber. Subsequently, Matrigel was diluted as 1:3 with serum-free DMEM medium, and added to the upper Transwell chamber (EMD Millipore, Billerica, MA, USA) and dried at room temperature. Following digestion with trypsin, the cells in each group were made into single cell suspensions using serum-free DMEM and starved for 24 h. Subsequently, cell suspension was added in the upper chamber with 200 and 500 μl DMEM medium (containing 10% FBS) were added to the 24-well plate. Subsequently, the chamber was put into each well and cultured for 48 h at 37°C. Subsequently, the chamber was taken out and washed using phosphate-buffered saline. The culture solution in the upper chamber was emptied. The residual Matrigel and cells on the micro-porous film of the chamber were wiped. The cells were fixed with 95% ethyl alcohol for 15 min and stained with 0.1% crystal violet at 37°C for 30 min and observed under an inverted microscope to record the mean number of cells passing through the basement membrane. Each experiment was repeated three times.

Tumor xenograft model of nude mice. The experimental animals used were 24 female BALB/C mice (4-6 weeks; mean body weight, 18±2 g), which were bought from the Institute of Laboratory Animal Sciences, Chinese Academy of Medical Sciences and Peking Union Medical College. The mice were fed at the Experimental Animal Center of Jingzhou Central Hospital and bred under specified
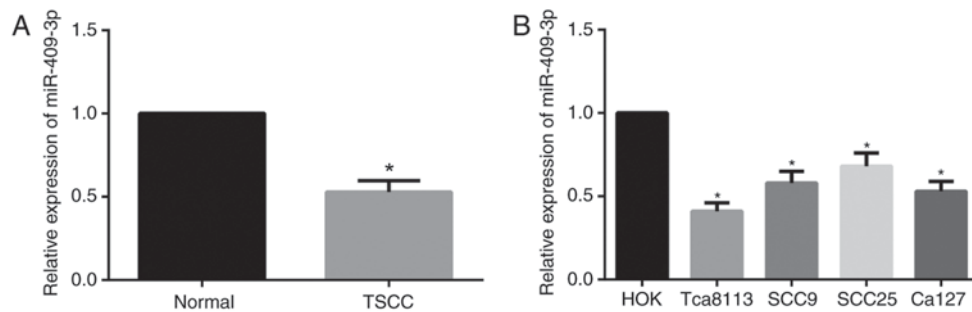
Figure 1. Expression of miR-409-3p in TSCC tissues and cell lines as detected by RT-qPCR. Relative expression of miR-409-3p in (A) normal controls and patients with TSCC by RT-qPCR. *P<0.05 vs. normal controls. Relative expression of miR-409-3p in (B) HOK and TSCC cell lines (Tca8113, SCC9, SCC25 and Ca127), as detected by RT-qPCR. *P<0.05 vs. HOK cells. HOK, human oral keratinocytes; miR, microRNA; RT-qPCR, reverse transcription-quantitative polymerase chain reaction; TSCC, tongue squamous cell carcinoma.

pathogen-free conditions (26°C, 70% relative humidity and a 12-h light/12-h dark cycle) in a germ-free environment with free access to food and water. The nude mice were divided into three groups with eight mice in each group, including blank group (inoculated with non-transfected Tca8113 cells), NC group (inoculated with Tca8113 cells transfected with NC sequence) and miR-409-3p mimic group (inoculated with Tca8113 cells transfected with miR-409-3p mimic). Subsequently, the cell concentration was adjusted to $5x10^6$/ml, and this was subcutaneously injected into the nude mice in each group at the right lingual margin with 0.05 ml/mouse. At the end of the fourth week, the mice were sacrificed by cervical dislocation, and tumor volume was calculated using the formula: Volume=(length/width^2)/2. Subsequently, the tumor tissue was separated, transplanted and weighted. Each axillary lymph node was fixed in 4% formaldehyde at 4°C for 12 h, embedded in paraffin and cut in 4 μm sections, examined and judged by two pathologists to determine whether lymph node metastasis was present. H&E staining and pathological examination were performed. Sections were stained for 3 min in 1:1 hematoxylin, and for 1 min in 0.5% eosin at room temperature. For immunohistochemistry, endogenous peroxidase was blocked by 3% H_2O_2 for 5 min at 37°C. The slide was blocked in 5% goat antiserum for 10 min at 37°C and incubated with lymphatic vessel endothelial hyaluronic acid receptor 1 (LYVE1; monoclonal anti-LYVE1 antibody; cat. no. sc-65647; Santa Cruz Biotechnology Inc., Dallas, TX, USA) at a dilution of 1:100 at 4°C overnight. The sections were then incubated with biotinylated secondary antibody (1:2,000) in a two-step detection reagent PV-6004 (OriGene Technologies, Inc., Beijing, China). Lymphatic microvessel density (LMVD) was determined as previously described by Weidner et al (26).

Statistical analysis. All data was analyzed using SPSS software (version 21.0; IBM Corp., Armonk, NY, USA) and expressed as the mean ± standard deviation. The comparison of normally distributed data between two groups were analyzed using unpaired t-tests, and the comparison among multiple groups was analyzed one-way analysis of variance followed by Tukey post hoc tests for multiple comparisons. The data are expressed as percentages and ratios. Discrete data were analyzed using a chi-square test. P<0.05 was considered to indicate a statistically significant difference.

Results

Expression of miR-409-3p in TSCC tissues and cell lines. RT-qPCR was carried out to detect miR-409-3p expression in TSCC tissues and cell lines. As demonstrated in Fig. 1, significant downregulation of miR-409-3p expression was demonstrated in tissues from patients with TSCC when compared with normal tongue mucosa tissues (P<0.05). Furthermore compared with the HOK cells, the expression of miR-409-3p was significantly decreased in TSCC cell lines (Tca8113, SCC9, SCC25 and Ca127; all P<0.05), and the most significant decrease in miR-409-3p expression was observed in Tca8113 cells (P<0.01), and therefore the subsequent *vitro* experiments were performed using Tca8113 cells.

Association between miR-409-3p expression and clinicopathological features of patients with TSCC. A significant association between miR-409-3p expression and lymph node metastasis and TNM stage was presented in Table II (all P<0.05). miR-409-3p expression was lower in patients with TSCC and lymph node metastasis and advanced TNM stages compared with those with no lymph node metastasis and with low TNM stages (Table II). However, no statistically significant difference was observed between miR-409-3p expression with age, sex, tumor diameter and differentiation of patients with TSCC (all P>0.05; Table II).

RDX is the target gene of miR-409-3p. Targetscan (www.targetscan.org/) was used to predict the target gene of miR-409-3p, and the miR-409-3p binding site within the 3'-UTR of *RDX* was identified (Fig. 2A). Furthermore, results from the dual-luciferase reporter gene assay revealed that following co-transfection with miR-409-3p mimic and *RDX* 3'UTR-WT, a decrease in the relative luciferase activity was present compared with the luciferase activity in cells that were co-transfected with miR-409-3p NC and *RDX* 3'UTR-WT (P<0.05). The luciferase activity in cells co-transfected with *RDX* 3'UTR-MUT + miR-409-3p NC and *RDX* 3'UTR-MUT + miR-409-3p mimic was not significantly different (P>0.05, Fig. 2A), suggesting that *RDX* may be a target gene of miR-409-3p.

Expression of miR-409-3p and RDX in various transfection groups. RT-qPCR and western blotting were conducted to determine the expression of miR-409-3p and RDX. In

Table II. Association between miR-409-3p expression and clinicopathological features of patients with tongue squamous cell carcinoma.

Clinicopathological features	n	miR-409-3p expression	P-value
Sex			0.710
Male	38	0.534±0.068	
Female	30	0.527±0.070	
Age			0.979
≥55	49	0.527±0.068	
<55	19	0.528±0.069	
Tumor diameter			0.869
≥2 cm	44	0.528±0.069	
<2 cm	24	0.531±0.069	
Differentiation			0.330
Moderately/poorly differentiated	42	0.521±0.075	
Well differentiated	26	0.538±0.057	
TNM stage			0.003
I-II	43	0.547±0.060	
III-IV	25	0.495±0.072	
Lymph node metastasis			<0.001
With	20	0.471±0.051	
Without	48	0.551±0.062	

miR, microRNA; TNM, tumor-node metastasis.

comparison with the blank group, no significant differences in miR-409-3p expression were exhibited in NC and si-RDX groups (both P>0.05; Fig. 2B). By contrast, an increase was demonstrated in miR-409-3p mimic group compared with the blank group. Furthermore, a marked decrease was detected in the miR-409-3p inhibitor and miR-409-3p inhibitor + si-RDX groups compared with the blank group (all P<0.05; Fig. 2B). As presented in Fig. 2C and D, the protein expression of RDX was significantly decreased in the miR-409-3p mimic and si-RDX groups compared with the blank group (both P<0.05; Fig. 2B). By contrast, an increase in RDX expression was detected in the miR-409-3p inhibitor group, compared with the blank group (P<0.05). When compared with the miR-409-3p inhibitor group, RDX protein expression was reduced in the miR-409-3p inhibitor + si-RDX group (P<0.05; Fig. 2B).

Proliferation of Tca8113 cells in each transfection group. Cell proliferation in each transfected group was detected using CCK-8 assay. No significant difference in cell proliferation was detected between the blank and NC groups (P>0.05; Fig. 3). However, compared with the blank group, cell proliferation was decreased in the miR-409-3p mimic and si-RDX groups respectively, and was increased in the miR-409-3p inhibitor group (all P<0.05; Fig. 3). Compared with the miR-409-3p inhibitor group, cell proliferation was decreased in the miR-409-3p inhibitor + si-RDX group (P<0.05; Fig. 3).

Migratory and invasive abilities of Tca8113 cells in each transfection group. Compared with the blank group, the migratory and invasive abilities of the cells in the NC group were not significant (both P>0.05; Fig. 4). There was a reduction in the miR-409-3p mimic and si-RDX groups and an increase in the miR-409-3p inhibitor group with respect to the migration and invasion abilities compared with the blank group (all P<0.05). Furthermore, a significant decrease in migratory and invasive abilities was detected in the miR-409-3p inhibitor + si-RDX group compared with the miR-409-3p inhibitor group (P<0.05, Fig. 4A and B).

Effects of miR-409-3p on tumor growth and lymphatic metastasis in nude mice. In order to further investigate the role of miR-409-3p *in vivo*, a tumor xenograft model in nude mice with Tca8113 cells was generated. The tumor formation rates of the nude mice in three groups were 100%. Following tumor inoculation, the tongue tumor presented outward growth with a marked increase in the number of blood vessels (Fig. 5Aa), and neck dissection demonstrated that the nude mice exhibited enlarged lymph nodes of the neck (Fig. 5Ab). Subsequently, the tumor volume and weight were measured at the end of the experiment. Compared with the blank group, tumor volume and weight were significantly reduced in the miR-409-3p mimic group (both P<0.05; Fig. 5B and C). There were no significances between the blank group and the NC group in terms of tumor volume and weight (both P>0.05; Fig. 5B and C).

Lymphatic metastasis in miR-409-3p mimic group was 0%, which was lower compared with the blank (6/8, 75%) and NC groups (7/8, 87.5%), data not shown. In addition, LMVD in each group was as follows: 8.36±1.12 for blank group, 8.92±1.26 for NC group, and 3.01±0.58 for the miR-409-3p mimic group (Fig. 5D). The LMVD in the miR-409-3p mimic group was significantly decreased compared with the blank group and the NC group (both P<0.05; Fig. 5D), suggesting that miR-409-3p mimic exerts inhibitory effects on lymphangiogenesis. H&E staining of tumor tissues is presented in Fig. 5E. The tumor cells appeared round or arranged in nest or sheet. In Fig. 5F, H&E staining results of a lymph node illustrated that tumor nest were present in lymph nodes, and the cell nuclei were darkly stained in unequal size. In Fig. 5G, the immunohistochemical staining indicated a strong brown positive staining of LYVE-1 in cytoplasm or cytomembrane.

Discussion

Recently, miR-409-3p was reported to be downregulated in various types of tumors. For instance, Cao *et al* (27) and Tang *et al* (28) reported that miR-409-3p may act as a promising prognostic indicator that is pronouncedly decreased in breast cancer and osteosarcoma respectively. miR-409-3p was also significantly associated with advanced TNM stage and metastasis, representing a poor prognosis. Consistently, in the present study, a significantly reduced expression of miR-409-3p was detected in TSCC tissues and cell lines compared with normal controls. miR-409-3p expression was lower in TSCC patients with lymph node metastasis and higher TNM stage compared with those without lymph node metastasis and lower TNM stage, suggesting miR-409-3p may act as a tumor suppressor in the progression of TSCC. Notably, Zhang *et al* (29) reported
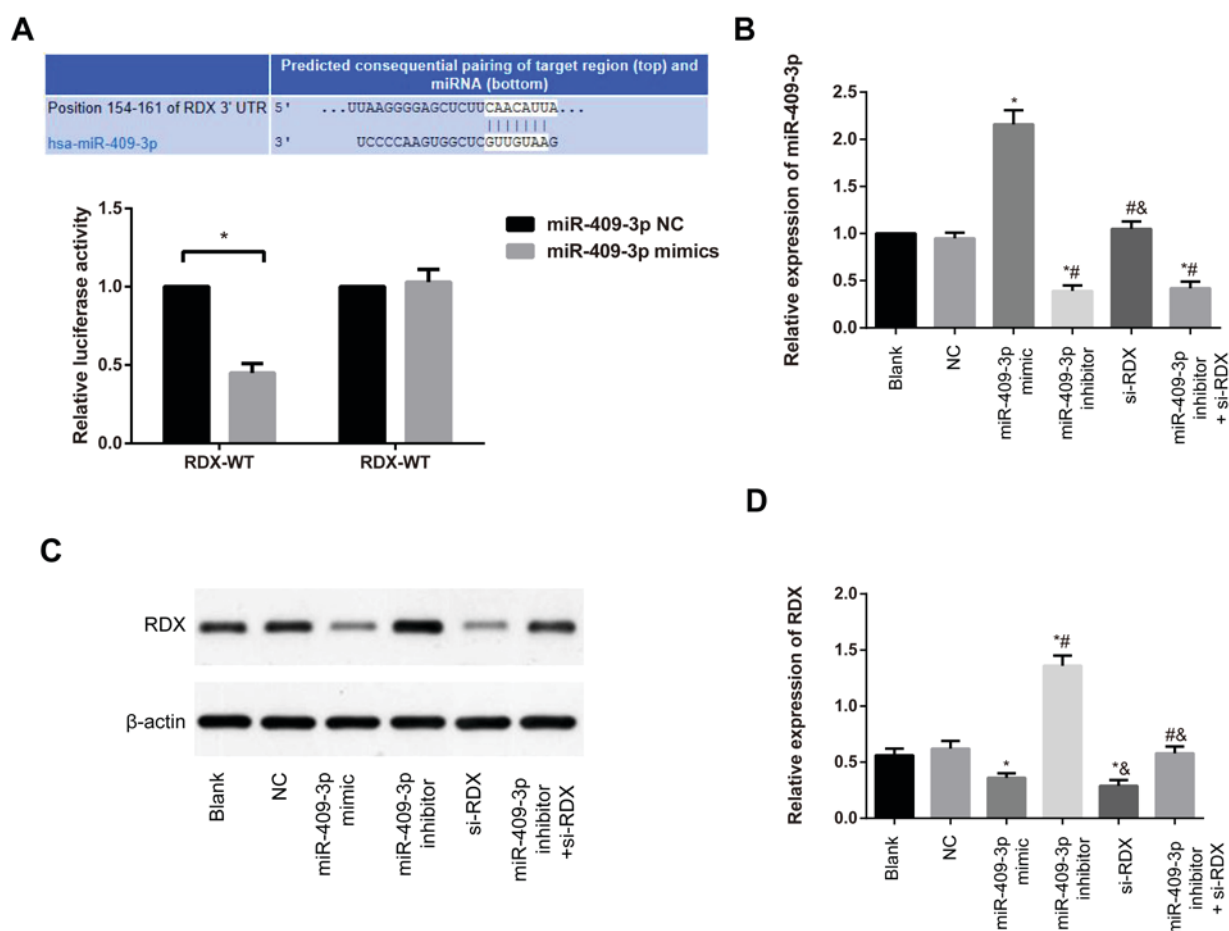
Figure 2. Predicted binding between miR-409-3p and *RDX*, and expression of miR-409-3p and RDX. (A) The binding sites of miR-409-3p in *RDX* 3'-UTR. miR-409-3p regulated the transcriptional activity of *RDX* as detected by dual-luciferase reporter gene assay. (B) Relative expression of miR-409-3p in each transfected group was detected by RT-qPCR. (C and D) Relative expression of RDX in each transfected group was detected by western blotting. *$P<0.05$ vs. blank group; #$P<0.05$ vs. miR-409-3p mimic group; &$P<0.05$ vs. miR-409-3p inhibitor group. miR, microRNA; NC, negative control; RDX, radixin; RT-qPCR, reverse transcription-quantitative polymerase chain reaction; si, small-interfering; TSCC, tongue squamous cell carcinoma; UTR, untranslated region; WT, wild-type.

an association between miR-409-3p and the suppression of breast cancer growth *in vitro* and *in vivo* partially via targeting *Akt1*. Additionally, E74 like ETS transcription factor 2 (*ELF2*) was demonstrated to be a novel direct target of miR-409-3p in osteosarcoma cells, where the overexpression of *ELF2* was able to rescue the suppressive function of miR-409-3p in cell proliferation and tumor growth (30).

Consistent with the aforementioned findings, *RDX* was identified as a target gene of miR-409-3p via dual-luciferase reporter gene assay in the present study. *RDX* is a type of cytoskeletal protein, which belongs to the ERM family (31). Notably, previous studies support that *RDX* serves an important role in the proliferation, migration, infiltration of tumor cells and the destruction of vascular endothelial barrier function (32,33), indicating that miR-409-3p might exert a tumor suppressor function during the development of TSCC via targeting *RDX*.

In the present study an *in vitro* experiment was performed using Tca8113 cells, and a decrease in *RDX* expression, cell proliferation, the number of invaded cells and migration distance following the transfection of miR-409-3p mimic or RDX siRNA were observed, suggesting that overexpression
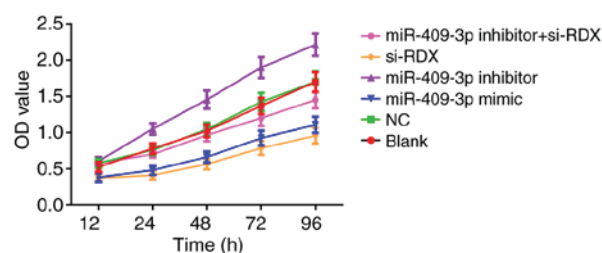

Figure 3. Cell proliferation of Tca8113 in each transfected group as detected by Cell Counting Kit-8 assay. miR, microRNA; NC, normal control; OD, optical density; RDX, radixin; si, small-interfering; TSCC, tongue squamous cell carcinoma.

of miR-409-3p and silencing of *RDX* are able to decrease the migratory and invasive abilities of TSCC cells to inhibit the growth of tumor cells.

Furthermore, it was also demonstrated that si-RDX is able to reverse the effect of miR-409-3p inhibitor in TSCC. Notably, a similar expression pattern of miR-409-3p and *RDX* was reported in gastric cancer, where miR-409-3p was able to suppress RDX expression via directly binding
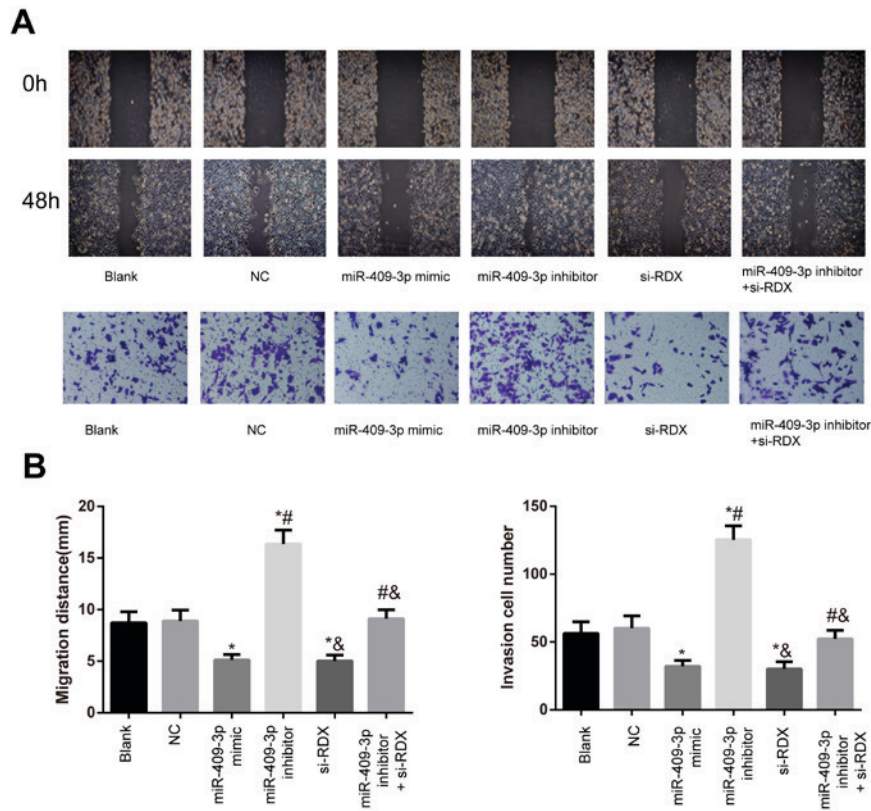
Figure 4. Migratory and invasive abilities of Tca8113 cells in each transfected group as detected by scratch wound-healing and Transwell invasion assays. (A) The migratory (upper panel) and invasive (bottom panel) abilities of Tca8113 cells were detected by scratch wound-healing assay and Transwell invasion assay, respectively (x200 magnification). (B) Quantification of the migration distance and the number of cells invaded in each treatment group. *P<0.05 vs. blank group; #P<0.05 vs. miR-409-3p mimic group; &P<0.05 vs. miR-409-3p inhibitor group miR, microRNA; NC, normal control; RDX, radixin; si, small-interfering; TSCC, tongue squamous cell carcinoma.
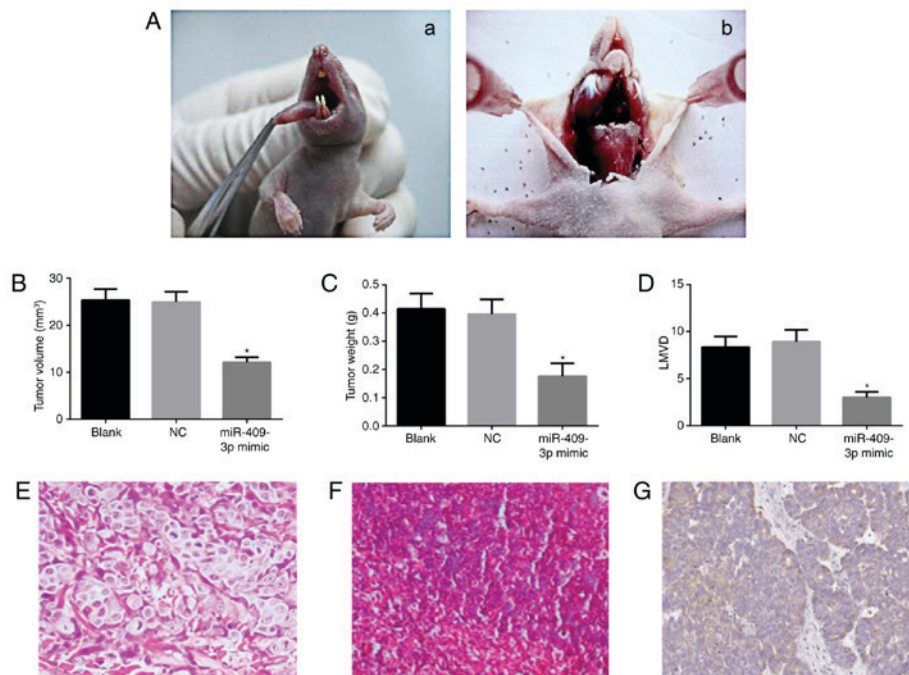

Figure 5. Effects of miR-409-3p on tumor growth and lymphatic metastasis in nude mice. (A) Representative images of tumor specimens in nude mice (a) The tongue tumor presented outward growth; (b) Bilaterally enlarged submandibular lymph nodes were present in the nude mice. Comparison of (B) tumor volume, and (C) weight of nude mice in each group. (D) Comparisons of LMVD measurements of nude mice in each group. (E) H&E staining of tumor tissues (magnification, x200) and (F) lymphatic metastasis in nude mice (magnification, x200). (G) Immunohistochemical staining of lymphatic vessel endothelial hyaluronan receptor 1 of tumor tissue (magnification, x200). *P<0.05 vs. the blank group. LMVD, Lymphatic microvessel density; miR, microRNA; NC, normal control; TSCC, tongue squamous cell carcinoma.

to its 3'-UTR region, thereby decreasing cell invasion and metastasis (20). Furthermore, the silencing of *RDX* in gastric cancer may inhibit the migration and invasion of SGC-7901 cells by upregulating E-cadherin expression, as indicated by Zhu *et al* (34), and the nuclear factor (NF)-κB/snail signaling pathway may also be involved. In addition, it was documented in a previous study that *RDX* is able to activate the Rac1-extracellular signal regulated kinase signaling pathway, and increase the secretion of matrix metallo-peptidase (MMP)-7, thereby decreasing the invasion and migration of colon cancer cells (35). Therefore, miR-409-3p is able to regulate the transduction of associated downstream signaling pathways via downregulating the expression of *RDX* and suppress the proliferative, invasive and migratory abilities of TSCC.

Due to the close association of the migratory and invasive abilities of tumor cells with their metastatic features (36), a tumor xenograft model of TSCC in nude mice was established with Tca8113 cells to investigate the role of miR-409-3p on tumor growth and lymphatic metastasis. It was demonstrated that a significant decrease in tumor volume, weight, lymphatic metastasis rate and LMVD was observed in the SCC nude mice that were transfected with miR-409-3p mimics compared with the blank group. The increase in LMVD was closely associated with lymphatic metastasis (37).

Current literature suggests that an increased LMVD indicates an increased risk for malignancies and a relatively poor prognosis (38). The present findings indicated that the overexpression of miR-409-3p exerted inhibitory effects on tumor growth and metastasis, which further confirms results of the *in vitro* experiments. In addition, it was previously reported that the overexpression of miR-409-3p in HT1080 cells was able to downregulate the expression of the target gene angiogenin so as to inhibit the growth of the transplantation tumor, angiogenesis and metastasis in nude mice (39). In pancreatic cancer cell line PANC-1, the inhibi-tion of *RDX* via small hairpin (sh)RNA was able to inhibit the proliferation and migration of cancer cells, and the tumor microvessel density was decreased so as to significantly inhibit the tumor growth following the implantation of *RDX* shRNA-transfected cells in nude mice (40). These findings suggest that the overexpression of miR-409-3p in nude mice may downregulate the expression of *RDX* and inhibit the metastasis of tumor cell.

In conclusion, the present findings indicated that miR-409-3p expression was decreased in TSCC tissues and cells compared with normal tongue mucosa tissues. miR-409-3p exerts a tumor inhibitory function, which delays cell proliferation by targeting *RDX*. This leads to the inhibition of migratory and invasive abilities of TSCC cells, providing a potential strategy for the treatment of TSCC.

Acknowledgements

Availability of data and materials

All data generated or analyzed during this study are included in this published article.

Authors' contributions

HC designed the study and performed experiments; JD analyzed the data and made the figures; HC and JD drafted and revised the paper; all authors approved the final version of the manuscript.

Ethics approval and consent to participate

The present study was approved by the Clinical Ethics Committee of Jingzhou Central Hospital (Hubei, China). All animal procedures were performed according to the Guide for the Care and Use of Laboratory Animals published by the US National Institutes of Health (22). All patients provided written informed consent to participate.

Consent for publication

All patients provided written informed consent for publication.

Competing interests

The authors declare that they have no competing interests.

References

1. Sannam Khan R, Khurshid Z, Akhbar S and Faraz Moin S: Advances of salivary proteomics in oral squamous cell carci-noma (OSCC) detection: An update. Proteomes 4: 2016.
2. Kidani K, Osaki M, Tamura T, Yamaga K, Shomori K, Ryoke K and Ito H: High expression of EZH2 is associated with tumor proliferation and prognosis in human oral squamous cell carci-nomas. Oral Oncol 45: 39-46, 2009.
3. Cao W, Feng Z, Cui Z, Zhang C, Sun Z, Mao L and Chen W: Up-regulation of enhancer of zeste homolog 2 is associated posi-tively with cyclin D1 overexpression and poor clinical outcome in head and neck squamous cell carcinoma. Cancer 118: 2858-2871, 2012.
4. Mücke T, Kanatas A, Ritschl LM, Koerdt S, Tannapfel A, Wolff KD, Loeffelbein D and Kesting M: Tumor thickness and risk of lymph node metastasis in patients with squamous cell carcinoma of the tongue. Oral Oncol 53: 80-84, 2016.
5. Kaboodkhani R, Karimi E, Khorsandi Ashtiani MT, Kowkabi S, Firouzifar MR, Yazdani F and Yazdani N: Evaluation of the correlation between CD44, tumor prognosis and the 5-Year survival rate in patients with oral tongue SCC. Iran J Otorhinolaryngol 28: 407-411, 2016.
6. Taghavi N and Yazdi I: Prognostic factors of survival rate in oral squamous cell carcinoma: Clinical, histologic, genetic and molecular concepts. Arch Iran Med 18: 314-319, 2015.
7. McIntire M and Redston M: Targeted therapies and predictive markers in epithelial malignancies of the gastrointestinal tract. Arch Pathol Lab Med 136: 496-503, 2012.
8. Djuranovic S, Nahvi A and Green R: A parsimonious model for gene regulation by miRNAs. Science 331: 550-553, 2011.
9. Hwang HW and Mendell JT: MicroRNAs in cell proliferation, cell death, and tumorigenesis. Br J Cancer 94: 776-780, 2006.
10. Shukla GC, Singh J and Barik S: MicroRNAs: Processing, maturation, target recognition and regulatory functions. Mol Cell Pharmacol 3: 83-92, 2011.
11. Bai R, Weng C, Dong H, Li S, Chen G and Xu Z: MicroRNA-409-3p suppresses colorectal cancer invasion and metastasis partly by targeting GAB1 expression. Int J Cancer 137: 2310-2322, 2015.

12. Wan L, Zhu L, Xu J, Lu B, Yang Y, Liu F and Wang Z: MicroRNA-409-3p functions as a tumor suppressor in human lung adenocarcinoma by targeting c-Met. Cell Physiol Biochem 34: 1273-1290, 2014.
13. Xu X, Chen H, Lin Y, Hu Z, Mao Y, Wu J, Xu X, Zhu Y, Li S, Zheng X and Xie L: MicroRNA-409-3p inhibits migration and invasion of bladder cancer cells via targeting c-Met. Mol Cells 36: 62-68, 2013.
14. Li C, Nie H, Wang M, Su L, Li J, Yu B, Wei M, Ju J, Yu Y, Yan M, et al: MicroRNA-409-3p regulates cell proliferation and apoptosis by targeting PHF10 in gastric cancer. Cancer Lett 320: 189-197, 2012.
15. Josson S, Gururajan M, Hu P, Shao C, Chu GY, Zhau HE, Liu C, Lao K, Lu CL, Lu YT, et al: miR-409-3p/-5p promotes tumorigenesis, epithelial-to-mesenchymal transition, and bone metastasis of human prostate cancer. Clin Cancer Res 20: 4636-4646, 2014.
16. Valastyan S, Chang A, Benaich N, Reinhardt F and Weinberg RA: Concurrent suppression of integrin alpha5, radixin, and RhoA phenocopies the effects of miR-31 on metastasis. Cancer Res 70: 5147-5154, 2010.
17. Liu G and Voyno-Yasenetskaya TA: Radixin stimulates Rac1 and Ca2+/calmodulin-dependent kinase, CaMKII: Cross-talk with Galpha13 signaling. J Biol Chem 280: 39042-39049, 2005.
18. Arpin M, Chirivino D, Naba A and Zwaenepoel I: Emerging role for ERM proteins in cell adhesion and migration. Cell Adh Migr 5: 199-206, 2011.
19. Tsai MM, Wang CS, Tsai CY, Chen CY, Chi HC, Tseng YH, Chung PJ, Lin YH, Chung IH, Chen CY and Lin KH: MicroRNA-196a/-196b promote cell metastasis via negative regulation of radixin in human gastric cancer. Cancer Lett 351: 222-231, 2014.
20. Zheng B, Liang L, Huang S, Zha R, Liu L, Jia D, Tian Q, Wang Q, Wang C, Long Z, et al: MicroRNA-409 suppresses tumour cell invasion and metastasis by directly targeting radixin in gastric cancers. Oncogene 31: 4509-4516, 2012.
21. The Helsinki Declaration of the World Medical Association (WMA). Ethical principles of medical research involving human subjects. polski merkuriusz lekarski: Organ Polskiego Towarzystwa Lekarskiego 36: 298-301, 2014.
22. Bayne K: Revised guide for the care and use of laboratory animals available. American physiological society. Physiologist 39: 199, 208-111, 1996.
23. Okuyemi OT, Piccirillo JF and Spitznagel E: TNM staging compared with a new clinicopathological model in predicting oral tongue squamous cell carcinoma survival. Head Neck 36: 1481-1489, 2014.
24. Livak KJ and Schmittgen TD: Analysis of relative gene expression data using real-time quantitative PCR and the 2(-Delta Delta C(T)) method. Methods 25: 402-408, 2001.
25. Ma Z, Li Y, Xu J, Ren Q, Yao J and Tian X: MicroRNA-409-3p regulates cell invasion and metastasis by targeting ZEB1 in breast cancer. IUBMB Life 68: 394-402, 2016.
26. Weidner N, Carroll PR, Flax J, Blumenfeld W and Folkman J: Tumor angiogenesis correlates with metastasis in invasive prostate carcinoma. Am J Pathol 143: 401-409, 1993.
27. Cao GH, Sun XL, Wu F, Chen WF, Li JQ and Hu WC: Low expression of miR-409-3p is a prognostic marker for breast cancer. Eur Rev Med Pharmacol Sci 20: 3825-3829, 2016.
28. Tang B, Liu C, Zhang QM and Ni M: Decreased expression of miR-490-3p in osteosarcoma and its clinical significance. Eur Rev Med Pharmacol Sci 21: 246-251, 2017.
29. Zhang G, Liu Z, Xu H and Yang Q: miR-409-3p suppresses breast cancer cell growth and invasion by targeting Akt1. Biochem Biophys Res Commun 469: 189-195, 2016.
30. Zhang J, Hou W, Jia J, Zhao Y and Zhao B: MiR-409-3p regulates cell proliferation and tumor growth by targeting E74-like factor 2 in osteosarcoma. FEBS Open Bio 7: 348-357, 2017.
31. Neisch AL and Fehon RG: Ezrin, radixin and moesin: Key regulators of membrane-cortex interactions and signaling. Curr Opin Cell Biol 23: 377-382, 2011.
32. Valderrama F, Thevapala S and Ridley AJ: Radixin regulates cell migration and cell-cell adhesion through Rac1. J Cell Sci 125: 3310-3319, 2012.
33. Yogesha SD, Sharff AJ, Giovannini M, Bricogne G and Izard T: Unfurling of the band 4.1, ezrin, radixin, moesin (FERM) domain of the merlin tumor suppressor. Protein Sci 20: 2113-2120, 2011.
34. Zhu YW, Yan JK, Li JJ, Ou YM and Yang Q: Knockdown of radixin suppresses gastric cancer metastasis in vitro by up-regulation of e-cadherin via NF-κB/snail pathway. Cell Physiol Biochem 39: 2509-2521, 2016.
35. Jiang QH, Wang AX and Chen Y: Radixin enhances colon cancer cell invasion by increasing MMP-7 production via Rac1-ERK pathway. ScientificWorldJournal 2014: 340271, 2014.
36. Courtneidge SA: Cell migration and invasion in human disease: The Tks adaptor proteins. Biochem Soc Trans 40: 129-132, 2012.
37. Eloy C, Santos J, Soares P and Sobrinho-Simões M: Intratumoural lymph vessel density is related to presence of lymph node metastases and separates encapsulated from infiltrative papillary thyroid carcinoma. Virchows Arch 459: 595-605, 2011.
38. Jardim JF, Francisco AL, Gondak R, Damascena A and Kowalski LP: Prognostic impact of perineural invasion and lymphovascular invasion in advanced stage oral squamous cell carcinoma. Int J Oral Maxillofac Surg 44: 23-28, 2015.
39. Weng C, Dong H, Chen G, Zhai Y, Bai R, Hu H, Lu L and Xu Z: miR-409-3p inhibits HT1080 cell proliferation, vascularization and metastasis by targeting angiogenin. Cancer Lett 323: 171-179, 2012.
40. Chen SD, Song MM, Zhong ZQ, Li N, Wang PL, Cheng S, Bai RX and Yuan HS: Knockdown of radixin by RNA interference suppresses the growth of human pancreatic cancer cells in vitro and in vivo. Asian Pac J Cancer Prev 13: 753-759, 2012.